The Degrees-of-Freedom in Monostatic ISAC Channels: NLoS Exploitation vs. Reduction

Shihang Lu, *Graduate Student Member, IEEE*, Fan Liu, *Member, IEEE*, Lajos Hanzo, *Life Fellow, IEEE*

***Abstract*—The degrees of freedom (DoFs) attained in monostatic integrated sensing and communications (ISAC) are analyzed. Specifically, monostatic sensing aims for extracting target-orientation information from the line of sight (LoS) channel between the transmitter and the target, since the Non-LoS (NLoS) paths only contain clutter or interference. By contrast, in wireless communications, typically, both the LoS and NLoS paths are exploited for achieving diversity or multiplexing gains. Hence, we shed light on the NLoS exploitation vs. reduction tradeoffs in a monostatic ISAC scenario. In particular, we optimize the transmit power of each signal path to maximize the communication rate, while guaranteeing the sensing performance for the target. The non-convex problem formulated is firstly solved in closed form for a single-NLoS-link scenario, then we harness the popular successive convex approximation (SCA) method for a general multiple-NLoS-link scenario. Our simulation results characterize the fundamental performance tradeoffs between sensing and communication, demonstrating that the available DoFs in the ISAC channel should be efficiently exploited in a way that is distinctly different from that of communication-only scenarios.**

***Index Terms*—ISAC, power allocation, parameter estimation, target detection, spatial degrees of freedom**

I. Introduction

In the forthcoming 5G-Advanced and 6G wireless networks, radio sensing at the network level has been considered as a beneficial new feature in support of emerging applications such as vehicle-to-everything (V2X) communications, as well as smart city and unmanned aerial vehicle (UAV) networks [1]. In the meantime, given the imminent spectrum crunch of wireless communications, the radar bands can be harnessed as alternative spectral resources. Owing to the commonalities between sensing and communication (S&C) in terms of hardware architecture and signal processing algorithms [2], Integrated Sensing and Communications (ISAC) constitutes a promising solution for embedding attractive radar sensing functionalities into the existing cellular infrastructure in a prompt and low-cost manner. Hence, it has received tremendous research attention in the recent years [3]–[8].

Conventional radar systems are conceived solely for optimizing the sensing performance without addressing the communication functionality [9]–[11]. With the emerging integration of S&C, both sensing-centric as well as communication-centric and joint designs are proposed for ISAC signal processing, which lead to flexible performance tradeoff between S&C [2]. In this spirit, novel resource allocation and waveform design approaches were developed [12] for approaching the ISAC performance bounds, leading to attractive integration and coordination gains [3]. More recently, numerous design tradeoffs have been revealed [2], ranging from information theoretical tradeoffs to physical layer tradeoffs [4], and to cross-layer designs [5].

While the aforementioned contributions relied upon sophisticated techniques, they generally assume that the S&C signals propagate over channels exhibiting similar statistical characteristics, even though in practical scenarios, things become more complex. Briefly, the presence of multiple paths can be exploited by the communication functionality. But not all the paths are useful for radar sensing [2]. Specifically, radar detection is typically more dependent on the direct line of sight (LoS) link between the radar transceiver and the target, since Non-LoS (NLoS) links typically contain unwanted clutter [11]. By contrast, wireless systems attain higher spatial degrees of freedom (DoFs) by exploiting both LoS and NLoS links. By noting this fundamental difference in S&C propagation channels, it is of pivotal importance to design efficient resource allocation for exploiting the spatial DoFs inherent within the ISAC channels, which motivates our research. To avoid confusion, the spatial DoFs in the ISAC channels of this compact letter refer to the total number of propagation paths.

Explicitly, we consider an ISAC base station (ISAC-BS) that supports a single communication user, which is also a target to be sensed. One typical example for such a scenario is the sensing-assisted vehicle-to-infrastructure (V2I) communication scenario, where a roadside unit (RSU) wishes to communicate with a vehicle, while simultaneously tracking its movement [3]. To be specific, we assume that there always exists a LoS link for target detection or tracking. Our aim is to design a novel power allocation (PA) strategy for balancing the fundamental performance tradeoff between the S&C spatial DoFs in this compact letter. Since unknown reflection coefficients may reduce the received signal energy to a level that does not allow reliable detection [9], the ISAC-BS estimates the reflection coefficient of each path first, and then judiciously share its total power across different paths through tailormade

This work was supported in part by Special Funds for the Cultivation of Guangdong College Students' Scientific and Technological Innovation ("Climbing Program" Special Funds, No. pdjh2022c0028), and in part by the National Natural Science Foundation of China under Grant 62101234, and in part by the Young Elite Scientist Sponsorship Program by CAST under Grant No. YESS20210055. L. Hanzo would like to acknowledge the financial support of the Engineering and Physical Sciences Research Council projects EP/W016605/1 and EP/P003990/1 (COALESCE) as well as of the European Research Council's Advanced Fellow Grant QuantCom (Grant No. 789028). (*Corresponding author: Fan Liu.*)

S. Lu and F. Liu are with the Department of Electronic and Electrical Engineering, Southern University of Science and Technology, Shenzhen 518055, China (email: lush2021@mail.sustech.edu.cn; liuf6@sustech.edu.cn).

L. Hanzo is with the Department of Electronics and Computer Science, University of Southampton, Southampton SO17 1BJ, UK (e-mail: lh@ecs.soton.ac.uk).

transmit beamforming (TBF).

In this compact letter, we shed light on a unique DoFs tradeoff of ISAC systems, namely, the associated propagation tradeoff. This kind of DoF tradeoff is very different from the classical communication-only scenario, where both the LoS and NLoS paths are communication-friendly. In ISAC systems, however, the NLoS paths are harmful for monostatic sensing, which has to be discussed further in terms of the NLoS reduction vs. exploitation tradeoff. Within this scope, the contributions of our work are summarized as follows:

- In addition to the V2I communication, our proposed system model can be readily extended to vehicle-to-vehicle (V2V) communication scenarios as well, where the rear vehicle wishes to communicate with the front vehicle while tracking its movement.
- To gain deeper insights into the PA design, we first consider the special case, where there is only a single NLoS link in addition to its LoS counterpart, and derive the optimal PA scheme in closed form.
- Then, we extend this special case into a multiple-NLoS-link scenario and provide a sub-optimal solution based on the popular successive convex approximation (SCA) algorithm.
- Our simulations characterize the performance tradeoff between S&C, which indicates that both the S&C performance can be simultaneously optimized by effectively exploiting all ISAC spatial DoFs.

II. System Model

We consider the downlink (DL) of a ISAC system, where the ISAC-BS is equipped with N_T transmit antennas (TAs) and N_R receive antennas (RAs) as shown in Fig. 1. The ISAC-BS is serving a single-antenna user (which is also treated as a point-like target) for simultaneously supporting S&C services. We assume that there are K channel impulse response (CIR) paths between the ISAC-BS and the target, only one of which is the LoS link. Let $\mathcal{K} \triangleq \{0, 1, \cdots, K-1\}$ denote the index set of the K propagation paths. We assume that the number K of propagation paths is *a-priori* known at the ISAC-BS, which may be accurately attained by angle estimation method, e.g., multiple signal classification (MUSIC) algorithm. For notational convenience, we do not distinguish between scatterers within each propagation path and clutter sources. As a consequence, the ISAC-BS receives signal reflections from multiple paths, where only the LoS path contains the target information of interest, and the echoes from the NLoS paths are treated as clutter.

To emphasize our main focus, here we also omit the propagation delays following [13], by assuming that we are employing a narrowband spatial model. In what follows, we elaborate on the S&C signal models.

A. Sensing Signal Model

Let $\mathbf{s} = [s_0, s_1, \ldots, s_{K-1}]^T \in \mathbb{C}^{K\times 1}$ denote the ISAC transmit signal vector with unit power symbol. Thus the echo

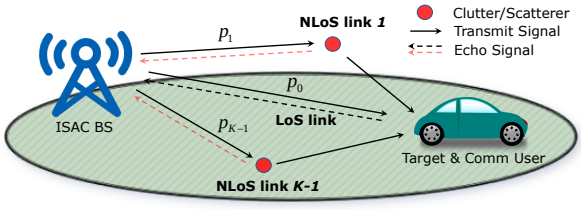

Fig. 1. Illustration of the system considered.

signal arriving at the ISAC-BS receiver can be expressed as

$$\mathbf{y}_r = \underbrace{\beta_0\sqrt{p_0}\mathbf{b}\left(\theta_0\right)\mathbf{a}^H\left(\theta_0\right)\mathbf{F}\mathbf{s}}_{\text{Target/LoS link}} + \underbrace{\sum_{k=1}^{K-1}\beta_k\sqrt{p_k}\mathbf{b}\left(\theta_k\right)\mathbf{a}^H\left(\theta_k\right)\mathbf{F}\mathbf{s}}_{\text{Path-dependent Clutter/NLoS links}} + \mathbf{z}_r, \quad (1)$$

where β_0 and $\{\beta_k\}_{k=1}^{K-1}$ are independent and identically distributed (iid) reflection coefficients of the target and the k-th clutter/scatterer source, while p_0 and p_k represent the transmit power to the LoS and NLoS links, θ_0 and θ_k are the angles of the target and the k-th path-dependent clutter source, $\mathbf{a}(\theta) = \frac{1}{\sqrt{N_T}}\left[1, e^{-j\pi\sin\theta}, \cdots, e^{-j\pi(N_T-1)\sin\theta}\right]^T$ and $\mathbf{b}(\theta) = \frac{1}{\sqrt{N_R}}\left[1, e^{-j\pi\sin\theta}, \cdots, e^{-j\pi(N_R-1)\sin\theta}\right]^T$ are the transmit and receive steering vectors, $\mathbf{F} = [\mathbf{f}_0, \mathbf{f}_1, \ldots, \mathbf{f}_{K-1}] \in \mathbb{C}^{N_T\times K}$ denotes the TBF matrix, and $\mathbf{z_r} \in \mathbb{C}^{N_R\times 1}$ represents the additive white Gaussian noise (AWGN) with variance of σ_R^2, respectively.

Following the standard assumption of the radar literature [9]–[11], and given the fact that we focus our attention on power sharing among multiple paths, we assume that the angle for each path is perfectly predicted/tracked. In our study, it is reasonable to choose the beamforming vector $\mathbf{f}_k$ for assuming that $\mathbf{a}^H(\theta_k)\mathbf{f}_k = 1$, which also implies that $\mathbf{a}^H(\theta_k)\mathbf{F}\mathbf{s} = s_k$ if the predicted angle perfectly matches the real angle [14]. By formulating multiple beams through the massive MIMO ISAC-BS, the symbol s_0 can be transmitted in the LoS link with the power p_0 and the symbol s_k can be mapped to the k-th NLoS path with the power p_k, respectively. After receive beamforming (RBF) at the ISAC-BS receiver, the sensing signal output of the receiving filter is given by

$$y_s = \beta_0\sqrt{p_0}\mathbf{w}^H\mathbf{b}\left(\theta_0\right)s_0 + \sum_{k=1}^{K-1}\beta_k\sqrt{p_k}\mathbf{w}^H\mathbf{b}\left(\theta_k\right)s_k + \mathbf{w}^H\mathbf{z}_r, \quad (2)$$

where $\mathbf{w}$ is the RBF vector designed for maximizing the signal-to-clutter-plus-noise ratio (SCNR). As a consequence, the SCNR can be written as

$$\begin{aligned}\text{SCNR} &= \frac{\left|s_0\beta_0\sqrt{p_0}\mathbf{w}^H\mathbf{b}\left(\theta_0\right)\right|^2}{\sum_{k=1}^{K-1}\left|s_k\beta_k\sqrt{p_k}\mathbf{w}^H\mathbf{b}\left(\theta_k\right)\right|^2 + \mathbf{w}^H\mathbf{w}\sigma_R^2} \\ &= \frac{\frac{p_0|s_0\beta_0|^2}{\sigma_R^2}\left|\mathbf{w}^H\mathbf{b}\left(\theta_0\right)\right|^2}{\mathbf{w}^H\left(\mathbf{\Sigma} + \mathbf{I}_{N_R}\right)\mathbf{w}}, \end{aligned} \quad (3)$$

where $\mathbf{\Sigma} = \sum_{k=1}^{K-1}\frac{p_k|s_k\beta_k|^2}{\sigma_R^2}\mathbf{b}\left(\theta_k\right)\mathbf{b}^H\left(\theta_k\right)$ and $\mathbf{I}_{N_R}$ is the N_R-dimensional identity matrix. We note that the NLoS/clutter components are regarded as interference and thus they are present in the denominator. We also assume that each transmit symbol s_k has unit power. The above SCNR maximization problem with respect to $\mathbf{w}$ is known as the minimum variance

distortionless response (MVDR) beamforming problem [11], which admits the closed-form solution of

$$\mathbf{w}^{\star}=\frac{\left[\mathbf{\Sigma}+\mathbf{I}_{N_R}\right]^{-1}\mathbf{b}\left(\theta_0\right)}{\mathbf{b}^H\left(\theta_0\right)\left[\mathbf{\Sigma}+\mathbf{I}_{N_R}\right]^{-1}\mathbf{b}\left(\theta_0\right)}. \tag{4}$$

By substituting $\mathbf{w}^{\star}$ of (4) into (3), the maximum achievable SCNR can be expressed in the form of

$$\mathrm{SCNR}=\frac{p_0\left|\beta_0\right|^2}{\sigma_R^2}\mathbf{b}^H\left(\theta_0\right)\left[\mathbf{\Sigma}+\mathbf{I}_{N_R}\right]^{-1}\mathbf{b}\left(\theta_0\right). \tag{5}$$

B. Communication Signal Model

Following the standard assumption in [12], we assume that the CIR is accurately obtained through channel estimation. The received communication signal composed with LoS and NLoS components at the target (which is also a communication user) is expressed as

$$y_c=\mathbf{h}^H\mathbf{F}\mathbf{s}+z_c, \tag{6}$$

where $\mathbf{h}\in\mathbb{C}^{N_T\times 1}$ represents the multiple-input-single-output (MISO) channel vector and z_c is the AWGN at the target with a variance of σ_C^2. Based on the Rician fading model, we have

$$\mathbf{h}=\sqrt{\frac{\varrho}{1+\varrho}}\mathbf{h}_{\mathrm{LoS}}+\sqrt{\frac{1}{1+\varrho}}\mathbf{h}_{\mathrm{NLoS}}, \tag{7}$$

where ϱ is the Rician factor and $\mathbf{h}_{\mathrm{LoS}}=\sqrt{p_0}\sqrt{N_T}\mathbf{a}\left(\theta_0\right)$ denotes the LoS component. The $K-1$ NLoS scattered components with may be expressed as $\mathbf{h}_{\mathrm{NLoS}}=\sum_{k=1}^{K-1}\sqrt{p_k}\sqrt{\frac{N_T}{K-1}}\alpha_k\mathbf{a}\left(\theta_k\right)$, where $\alpha_k\sim\mathcal{CN}(0,1)$ is the complex path gain. Based on (6), the communication signal-to-noise ratio (SNR) is written as

$$\mathrm{SNR}=\frac{\left|\mathbf{h}^H\mathbf{F}\mathbf{s}\right|^2}{\sigma_c^2}=\frac{\left|\sum_{k=0}^{K-1}\sqrt{p_k}\tilde{x}_k\right|^2}{\sigma_c^2}, \tag{8}$$

where $\tilde{x}_0=\sqrt{\frac{N_T\varrho}{1+\varrho}}s_0$ and $\{\tilde{x}_k\}_{k=1}^{K-1}=\sqrt{\frac{N_T}{(K-1)(1+\varrho)}}\alpha_k s_k$.

C. Parameter Estimation

Since all $\{\beta_k\}_{k=0}^{K-1}$ coefficients are unknown but iid, the ISAC-BS has to estimate $\{\beta_k\}_{k=0}^{K-1}$ from different paths and then judiciously allocate the transmit power based on all estimated parameters in the first epoch, while the ISAC-BS performs target detection in the second epoch. Again, we assume that $\{\beta_k\}_{k=0}^{K-1}$ are iid; and subject to $\mathcal{CN}(0,\sigma^2)$ [9]. Then, based on (1), the corresponding Linear Bayesian Estimation model at sample n is given by

$$\mathbf{y}_r[n]=\mathbf{H}[n]\boldsymbol{\beta}+\mathbf{z}_r[n], n=1\ldots N, \tag{9}$$

where the k-th column of $\mathbf{H}[n]$ is $\sqrt{p}s_k[n]\mathbf{b}\left(\theta_k\right)$, while $p=P_T/K$ denotes the initial transmit power used for estimation, and $[\boldsymbol{\beta}]_k=\beta_k$ represents the parameters to be estimated. Finally, N is the number of sampling snapshots, respectively. By stacking the signal snapshots observed into a single vector, the estimation model becomes

$$\mathbf{y}=\mathbf{H}\boldsymbol{\beta}+\mathbf{z}, \tag{10}$$

$$\text{where }\mathbf{y}=\begin{bmatrix}\mathbf{y}_r\left[1\right]\\ \mathbf{y}_r\left[2\right]\\ \vdots\\ \mathbf{y}_r\left[N\right]\end{bmatrix},\mathbf{H}=\begin{bmatrix}\mathbf{H}\left[1\right]\\ \mathbf{H}\left[2\right]\\ \vdots\\ \mathbf{H}\left[N\right]\end{bmatrix},\mathbf{z}=\begin{bmatrix}\mathbf{z}_r\left[1\right]\\ \mathbf{z}_r\left[2\right]\\ \vdots\\ \mathbf{z}_r\left[N\right]\end{bmatrix}.$$

Note that $\boldsymbol{\beta}\sim\mathcal{CN}(\mathbf{0},\sigma^2\mathbf{I}_K)$ and $\mathbf{z}\sim\mathcal{CN}(\mathbf{0},\sigma_R^2\mathbf{I}_{NN_R})$. Therefore, the minimum mean square error (MMSE) estimator of $\boldsymbol{\beta}$ can be readily constructed as [15]

$$\hat{\boldsymbol{\beta}}=\left(\frac{\sigma_R^2}{\sigma^2}\mathbf{I}_K+\mathbf{H}^H\mathbf{H}\right)^{-1}\mathbf{H}^H\mathbf{y}. \tag{11}$$

With the estimate (11) at hand, we approximate the SCNR as

$$\mathrm{SCNR}_{\mathrm{est}}=p_0\gamma_0\mathbf{b}^H\left(\theta_0\right)\left[\mathbf{\Sigma}_{\mathrm{est}}+\mathbf{I}_{N_R}\right]^{-1}\mathbf{b}\left(\theta_0\right), \tag{12}$$

where $\mathbf{\Sigma}_{\mathrm{est}}=\sum_{k=1}^{K-1}p_k\gamma_k\mathbf{b}\left(\theta_k\right)\mathbf{b}^H\left(\theta_k\right)$ and $\gamma_k=\frac{\left|\hat{\beta}_k\right|^2}{\sigma_R^2}, k\in\mathcal{K}$. Since random fading may reduce the received signal energy [9], We first have to identify whether the target is present or absent, as detailed in the following.

D. Target Detection

We now proceed by constructing a hypothesis test, where we seek to choose between two hypotheses, i.e. $\mathcal{H}_1$, target present, or $\mathcal{H}_0$, target absent. This can be expressed as

$$y=\begin{cases}\mathcal{H}_0:\sum_{k=1}^{K-1}y_k+z,\\ \mathcal{H}_1:y_0+\sum_{k=1}^{K-1}y_k+z,\end{cases} \tag{13}$$

where $y_k=\frac{\sqrt{p_k}\beta_k\mathbf{w}^H\mathbf{b}(\theta_k)}{\sqrt{N}}\sum_{n=1}^{N}s_k[n]s_0^*[n], k\in\mathcal{K}$, $z=\frac{1}{\sqrt{N}}\sum_{n=1}^{N}\mathbf{w}^H\mathbf{z}_r[n]s_0^*[n]$ and $\frac{1}{\sqrt{N}}s_0^*[n]$ is the matching signal. Here $1/\sqrt{N}$ is set for ensuring that the received signal energy remains constant after matched filtering. By noting that $\beta_k\sim\mathcal{CN}(0,\sigma^2)$ and $z\sim\mathcal{CN}(0,\|\mathbf{w}\|^2\sigma_R^2)$, we have $y|\mathcal{H}_0\sim\mathcal{CN}(0,\eta_0)$ and $y|\mathcal{H}_1\sim\mathcal{CN}(0,\eta_1)$, where $\eta_0=\sum_{k=1}^{K-1}p_k|\mathbf{w}^H\mathbf{b}\left(\theta_k\right)|^2\sigma^2+\|\mathbf{w}\|^2\sigma_R^2$ and $\eta_1=\sum_{k=0}^{K-1}p_k|\mathbf{w}^H\mathbf{b}\left(\theta_k\right)|^2\sigma^2+\|\mathbf{w}\|^2\sigma_R^2$. Based on the above, we can now formulate the Neyman-Pearson detector [15]

$$T=|y|^2\underset{\mathcal{H}_0}{\overset{\mathcal{H}_1}{\gtrless}}\delta, \tag{14}$$

in which the threshold δ is set to satisfy the maximum tolerant probability of false alarm P_{FA}. Thus the value of T is distributed as $T|\mathcal{H}_0\sim\frac{\eta_0}{2}\chi_2^2$ and $T|\mathcal{H}_1\sim\frac{\eta_1}{2}\chi_2^2$, respectively, where χ_2^2 denotes the central chi-squared distribution having a DoF $=2$.

Given a constant P_{FA}, it follows that δ can be set to [9] $\delta=\frac{\eta_0}{2}F_{\chi_2^2}^{-1}\left(1-P_{\mathrm{FA}}\right)$, where $F_{\chi_2^2}^{-1}$ denotes the inverse cumulative distribution function of the chi-square distribution. Accordingly, the probability of correct detection P_D is [9]

$$P_D=\mathbb{P}(T>\delta|\mathcal{H}_1)=1-F_{\chi_2^2}\left(\frac{\eta_0}{\eta_1}F_{\chi_2^2}^{-1}\left(1-P_{\mathrm{FA}}\right)\right). \tag{15}$$

III. Problem Formulation and solution

In this section, we discuss the PA problem across multiple propagation paths. Our aim is to exploit ISAC channel as DoFs tradeoff for maximizing the communication performance, while still satisfying the sensing performance.

A. Optimization Problem Formulation

It is provable that P_D is monotonically decreasing with η_0/η_1, i.e., $P_D\propto\mathrm{SCNR}$, both of which are determined by the specific PA. Therefore, to constrain P_D is equivalent to constraining the SCNR. In what follows, we choose SCNR as our sensing performance metric. By employing the achievable

communication rate as our objective function, the PA problem can be formulated as

$$\max_{\mathbf{p}} \quad \log_2(1+\mathrm{SNR}) \tag{16a}$$

$$\text{s.t.} \quad \mathrm{SCNR}_{\mathrm{est}} \geq \Gamma, \tag{16b}$$

$$\mathbf{1}^T\mathbf{p} \leq P_T, p_k \geq 0, \forall k \in \mathcal{K}, \tag{16c}$$

where $\mathbf{p} = [p_0, p_1, \ldots, p_{K-1}]^T$ is the PA vector to be optimized, $\Gamma > 0$ is the minimum required SCNR, and P_T is the total transmit power budget. It can be readily seen that equality holds for $\mathbf{1}^T\mathbf{p} \leq P_T$, when the optimum is reached. By noting (8), problem (16) can be equivalently recast as

$$\max_{\mathbf{p}} \quad \left|\sum_{k=0}^{K-1}\sqrt{p_k}\tilde{x}_k\right|^2 \tag{17a}$$

$$\text{s.t.} \quad \mathrm{SCNR}_{\mathrm{est}} \geq \Gamma, \tag{17b}$$

$$\mathbf{1}^T\mathbf{p} = P_T, p_k \geq 0, \forall k \in \mathcal{K}. \tag{17c}$$

Since we assume that the communication CIR is perfectly known at the ISAC-BS [3], [4], one can simply compensate for both the phases of the complex path gain factor α_k and the complex transmit signals s_k via the following modification of the TBF matrix

$$\mathbf{F} = \left[\mathbf{f}_0 e^{-jg_0}, \mathbf{f}_1 e^{-jg_1}, \ldots, \mathbf{f}_{K-1}e^{-jg_{K-1}}\right], \tag{18}$$

where $g_0 = \angle s_0$ represents the phase of the complex transmit symbol in the LoS link, and $g_k = \angle\alpha_k s_k, k = 1, \ldots, K-1$, denotes the phase of the complex path gain factor and the complex transmit symbol in the k-th NLoS link, respectively. Based on (18), we have $\mathbf{a}^H(\theta_0)\mathbf{F}\mathbf{s} = |s_0|$ and $\alpha_k\mathbf{a}^H(\theta_0)\mathbf{F}\mathbf{s} = |\alpha_k s_k|, k = 1, \ldots, K-1$. We remark that the modified TBF matrix $\mathbf{F}$ does not affect the radar SCNR. Accordingly, we can reformulate problem (17) as

$$\max_{\mathbf{p}} \quad \sum_{k=0}^{K-1}\sqrt{p_k}x_k \quad \text{s.t. (17b) and (17c)}, \tag{19}$$

where $x_0 = \sqrt{\frac{N_T\varrho}{1+\varrho}}|s_0|$ and $\{x_k\}_{k=1}^{K-1} = \sqrt{\frac{N_T}{(K-1)(1+\varrho)}}|\alpha_k s_k|$.

However, problem (19) is still non-convex, since (17b), which is expressed as a convex function greater than a given threshold, is non-convex. This makes it challenging for us to design an efficient solver for (19). More particularly, dealing with the non-convex constraint (17b) is quite challenging. To gain deeper insights here, we consider a pair of cases having different numbers of NLoS propagation paths, a.k.a., clutter sources. Specifically, a single NLoS link ($K = 2$) and multiple NLoS links ($K > 2$) are considered.

B. Single NLoS Link Case

Firstly, we assume that there are only two channel links, i.e. CIR taps between the ISAC-BS and the target. In this case, problem (19) can be simplified to

$$\max_{\{p_0,p_1\}} \quad \sqrt{p_0}x_0 + \sqrt{p_1}x_1 \tag{20a}$$

$$\text{s.t.} \quad p_0\gamma_0\mathbf{b}^H(\theta_0)\left[\mathbf{\Sigma}(p_1) + \mathbf{I}_{N_R}\right]^{-1}\mathbf{b}(\theta_0) \geq \Gamma, \tag{20b}$$

$$p_0 + p_1 = P_T, p_0 \geq 0, p_1 \geq 0, \tag{20c}$$

where $\mathbf{\Sigma}(p_1) = p_1\gamma_1\mathbf{b}(\theta_1)\mathbf{b}^H(\theta_1)$. Note that (20) is a non-convex optimization problem which is difficult to solve directly. Thanks to Woodbury's matrix identity [15], we have

$$\left[\mathbf{\Sigma}(p_1) + \mathbf{I}_{N_R}\right]^{-1} = \mathbf{I}_{N_R} - \frac{p_1\gamma_1}{p_1\gamma_1+1}\mathbf{b}(\theta_1)\mathbf{b}^H(\theta_1). \tag{21}$$

Then, by substituting (20c) and (21) into (20b), we have

$$h(p_1) \triangleq Ap_1^2 + Bp_1 + C \leq 0, \tag{22}$$

where $A = (1-b)\gamma_0\gamma_1$, $B = \Gamma\gamma_1 + \gamma_0 + P_T(b-1)\gamma_0\gamma_1$, $C = \Gamma - P_T\gamma_0$, $b = \mathbf{b}^H(\theta_0)\mathbf{b}(\theta_1)\mathbf{b}^H(\theta_1)\mathbf{b}(\theta_0)$. After the above derivation, we have the following equivalent constraint as for (20b) and (20c)

$$0 \leq p_1 \leq \min\{P_A, P_T\}, \tag{23}$$

where P_A is the positive root of $h(p_1) = 0$, whose expression is omitted here. Thus, problem (20) can be reformulated as

$$\max_{p_1} \quad f(p_1) \quad \text{s.t.} \quad 0 \leq p_1 \leq \min\{P_A, P_T\}, \tag{24}$$

where we have $f(p_1) = \sqrt{P_T - p_1}x_0 + \sqrt{p_1}x_1$. It is not difficult to show that (P24) boils down to a one-dimensional optimization problem associated with a given feasible interval. The optimal solution $p_1^\star$ can be readily expressed as:

$$p_1^\star = \arg\max_{\mathcal{D}} \ f(p_1), \tag{25}$$

where $\mathcal{D} = \{\min\{P_A, P_B\}, 0\}$ denotes the set of boundary points and extreme point of the objective function. Here the extreme point $P_B = \frac{P_T x_1^2}{x_0^2+x_1^2}$ can be calculated by solving $f'(p_1) = \frac{-\frac{1}{2}x_0}{\sqrt{P_T-p_1}} + \frac{\frac{1}{2}x_1}{\sqrt{p_1}} = 0$.

C. Multiple NLoS Links

Now we investigate the multiple-NLoS-link scenario by tackling the non-convex constraint (17b) in (19). For notational convenience, we let $g(\mathbf{p}_c) = \mathbf{b}^H(\theta_0)\left[\mathbf{\Sigma}_{\mathrm{est}} + \mathbf{I}_{N_R}\right]^{-1}\mathbf{b}(\theta_0)$, where $\mathbf{p}_c = [p_1, p_2, \ldots, p_{K-1}]^T \in \mathbb{R}^{K-1}$ represents the transmit power vector with each element respectively the power allocated to each NLoS link. It is worth pointing out that the SCA method proposed in [16] cannot be directly applied in our optimization problem, since the slack conditions have to be addressed case-by-case. To tackle this issue, we first show that $g(\mathbf{p}_c)$ is convex with respect to $\mathbf{p}_c$, which provides a necessary condition for applying the SCA technique to tackle the non-convex constraint (17b). Then, we recast the original optimization problem into a convex program, which can be solved in an iterative manner.

It is plausible that $g(\mathbf{p}_c)$ is convex with respect to $\mathbf{p}_c$ by its convex Epigraph [17], which is given by (26).

To this end, observe that any convex function is globally lower-bounded by its first-order Taylor expansion at any point [17], thus the lower bound of $g(\mathbf{p}_c)$ is formulated as

$$g(\mathbf{p}_c) \geq g_{lb}(\mathbf{p}_c) \triangleq g(\mathbf{p}_c^r) + (\nabla g(\mathbf{p}_c^r))^T(\mathbf{p}_c - \mathbf{p}_c^r), \tag{27}$$

where $\mathbf{p}_c^r$ is the point given at the r-th iteration and $\nabla g(\mathbf{p}_c^r)$ is the gradient vector at $\mathbf{p}_c^r$. The k-th element of $\nabla g(\mathbf{p}_c^r)$ is $-\mathbf{b}^H(\theta_0)\left[\mathbf{\Sigma}_{\mathrm{est}}^r + \mathbf{I}_{N_R}\right]^{-1}\mathbf{B}_k\left[\mathbf{\Sigma}_{\mathrm{est}}^r + \mathbf{I}_{N_R}\right]^{-1}\mathbf{b}(\theta_0)$, where $\mathbf{\Sigma}_{\mathrm{est}}^r = \sum_{k=1}^{K-1}p_k^r\gamma_k\mathbf{b}(\theta_k)\mathbf{b}^H(\theta_k)$ is a constant matrix at the r-th iteration and $\mathbf{B}_k = \mathbf{b}(\theta_k)\mathbf{b}^H(\theta_k)$. By introducing the SCA technique, we can thus formulate a sub-problem in each iteration as

$$\begin{aligned}\mathbf{epi}\ g = &\left\{(\mathbf{p}_c, t) \mid \mathbf{p}_c \in \mathrm{dom}\ g, \mathbf{b}^H(\theta_0)\left[\sum_{k=1}^{K-1}\gamma_k p_k \mathbf{b}(\theta_k)\mathbf{b}^H(\theta_k) + \mathbf{I}_{N_R}\right]^{-1}\mathbf{b}(\theta_0) \leqslant t\right\} \\ \Longleftrightarrow &\left\{(\mathbf{p}_c, t) \mid \mathbf{p}_c \in \mathrm{dom}\ g, \begin{bmatrix} t & \mathbf{b}^H(\theta_0) \\ \mathbf{b}(\theta_0) & \sum_{k=1}^{K-1}\gamma_k p_k \mathbf{b}(\theta_k)\mathbf{b}^H(\theta_k) + \mathbf{I}_{N_R}\end{bmatrix} \succeq \mathbf{0}\right\}.\end{aligned} \tag{26}$$

$$\begin{aligned}\max_{p_0, \mathbf{p}_c}\ &\sum_{k=0}^{K-1}\sqrt{p_k}x_k \\ \text{s.t.}\ \ &g_{lb}(\mathbf{p}_c) - \frac{\Gamma}{\gamma_0 p_0} \geq 0, \ \text{and (17c)}.\end{aligned} \tag{28}$$

Observe that problem (28) is convex and thus can be solved by CVX directly [16], [17]. Therefore, the original optimization problem (19) can be solved in an iterative manner, which is characterized in **Algorithm** 1.

Let us denote the total maximum number of iterations required in **Algorithm** 1 by $r_{\max}$. In each iteration, the convex optimization problem (19) is solved via the standard interior-point method of the complexity of $\mathcal{O}(K^{3.5})$ [17]. As a result, the overall complexity of **Algorithm** 1 is in a polynomial order of $\mathcal{O}(r_{\max}K^{3.5})$.

Algorithm 1 SCA-Based Power Allocation.

Input: $P_T, \alpha_k, \sigma_R^2, \sigma_C^2, \theta_0, \theta_k, N_T, N_R, K, r_{\max}, \epsilon$.
Output: $\mathbf{p}$.

1: Initialize the transmit power $\mathbf{p}^r$, r = 1.
2: Initialize the estimated reflecting coefficients by (11).
3: **repeat**
4: Calculate $\nabla g(\mathbf{p}_c^r)$.
5: Solve problem (28) for given $\mathbf{p}^r$. Denote the optimal solution as $\mathbf{p}^{r+1}$.
6: Update $r = r + 1$.
7: **until** The increase of the objective value is below $\epsilon = 10^{-5}$ or $r = r_{\max}$.

IV. Simulation Results

In this section, we evaluate the proposed algorithm by MonteCarlo based simulation results. Without loss of generality, the reflecting coefficients β_k, and the complex channel gain α_k are assumed to obey the standard Complex Gaussian distribution $\mathcal{CN}(0,1)$ and the Rician factor is set as $\varrho = 1$. Unless otherwise specified, the maximum transmit power is given as $P_T = 20$ dBm and the noise power is set as $\sigma_c^2 = \sigma_r^2 = 0$ dBm. The target is located at $\theta_0 = 0°$ (LoS link) and the clutter sources (NLoS links) are located at $\theta_1 = -20°, \theta_2 = -10°, \theta_3 = 10°, \theta_4 = 20°$, respectively. The SCNR threshold Γ spans from 0 dB to Γ_T dB, where $\Gamma_T = P_T\gamma_0$ is the maximum SCNR threshold amputated for avoiding an infeasible case.

We commence by evaluating the S&C performance under different DoFs in Fig. 2 through the proposed approaches, using one pair of benchmarks, namely,

- Sensing-centric (SC) design, which reaches the best sensing performance by setting $p_0 = P_T$, i.e., the ISAC-BS allocates all the power to the LoS link;

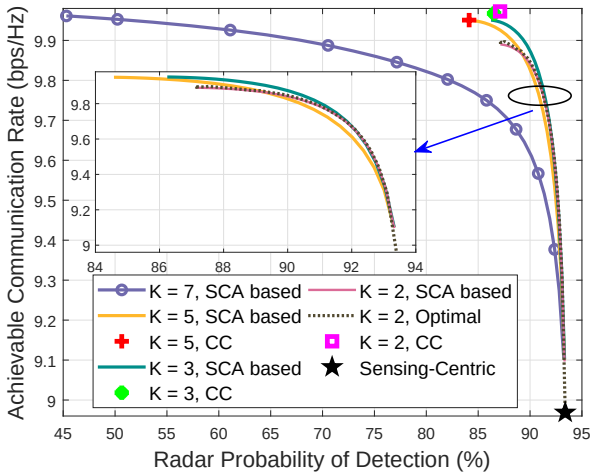

Fig. 2. S&C performance tradeoff.

- Communication-centric (CC) design, which reaches the maximum achievable communication rate by applying the Cauchy-Schwarz inequality to the objective function of (28), i.e., $(\sum_{k=0}^{K-1}\sqrt{p_k}x_k)^2 \leq P_T(\sum_{k=0}^{K-1}x_k^2)$.

First, we observe that the SCA-based method approaches the optimal solution for $K = 2$, because the SCA technique reduces the feasible region. Then, we also see that regardless of the spatial DoFs, the achievable maximum radar probability of detection is identical for all cases since the ISAC-BS assigns its total power to the LoS link. By contrast, when the spatial DoFs are higher, our approach usually attains a higher communication rate (see $K = 2$, $K = 3$, $K = 5$ and $K = 7$ in Fig. 2). But this is not always true, when we also take the sensing performance into consideration, especially when the radar probability of detection has to be above 90%. This is because having higher DoFs for communications imposes more clutter sources, which are harmful to radar sensing. Futhermore, all proposed schemes are capable of attaining a flexible CC or SC tradeoff by adjusting the PA among different paths. Again, CC design exploits all available spatial DoFs, while SC design only relies on LoS transmission. We can conclude through Fig. 2 that utilizing flexible spatial DoFs tradeoff is important for achieving scalable S&C performance.

In Fig. 3, we characterize our PA scheme for $K = 5$ and $K = 2$ respectively based **Algorithm** 1. Observe that upon increasing the SCNR threshold, the transmit power allocated to the NLoS links is reduced. When the SCNR approaches Γ_T, i.e., the maximum feasibility threshold, the transmit power allocated to the LoS link tends to approach P_T for satisfying more strict SCNR threshold requirements. Futhermore, since we assume that both the reflecting coefficients and the complex

channel gain are iid, the transmit power of different NLoS links is commensurate (see $K = 5$ in Fig. 3(a)).

Finally, in Fig. 4, we show the S&C performance tradeoff vs. P_T, for $K = 5$. The maximum achievable communication rate and the probability of successful detection increase with the maximum transmit power budget. Moreover, the S&C performance region is also extended upon increasing the power budget.

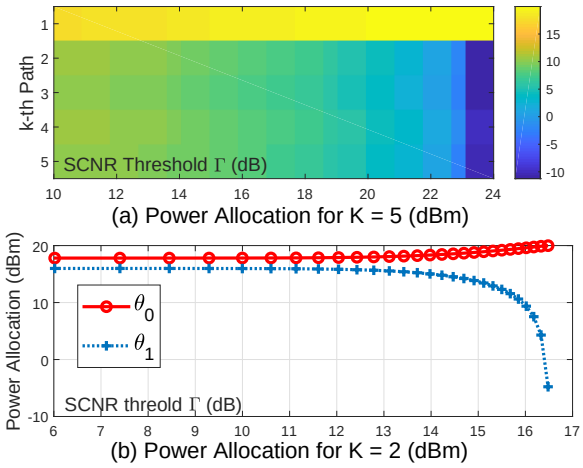

Fig. 3. PA with $K = 5$ and $K = 2$.

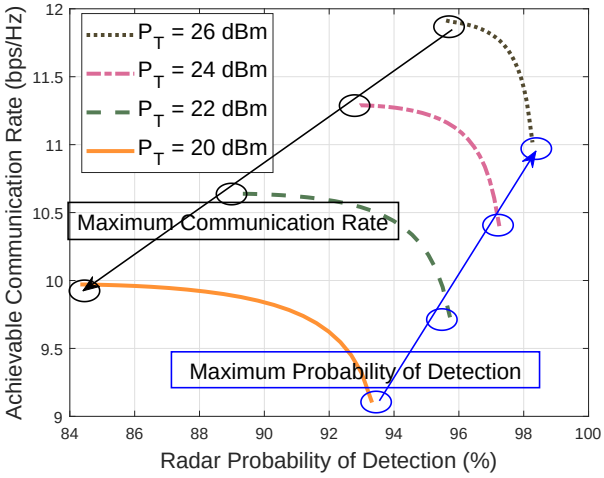

Fig. 4. S&C performance versus P_T.

V. Conclusions

In this compact letter, we investigated the S&C performance tradeoffs in terms of the ISAC channel's DoFs, by proposing a novel transmit power allocating accords the transmit signal propagation paths. We first constructed the parameter estimator and target detector under the signal model considered. Then, we formulated a PA problem for maximizing the achievable communication rate subject to a minimal required radar SCNR constraint and power budget. To gain deeper insights into the problem, the closed-form solution was focused for the case of a single NLoS link. Then, we extended it to the more practical scenario of multiple NLoS links. To tackle the resultant non-convex optimization problem, we harnessed the SCA algorithm, where the transmit power vector is optimized in an iterative manner. Finally, simulation results were provided for characterizing the performance tradeoff between S&C, which suggests that both the S&C performance can be simultaneously optimized by exploiting all ISAC spatial DoFs. The results obtained from this research indicate that, in a practical ISAC system, one can arrange for the optimized transmit power sharing among LoS and NLoS paths to strike different performance tradeoffs and meet the demanding requirements of both sensing and communications.

References

[1] Y. Cui, F. Liu, X. Jing, and J. Mu, "Integrating sensing and communications for ubiquitous IoT: Applications, trends, and challenges," *IEEE Network*, vol. 35, no. 5, pp. 158–167, 2021.

[2] F. Liu, Y. Cui, C. Masouros, J. Xu, T. X. Han, Y. C. Eldar, and S. Buzzi, "Integrated sensing and communications: Towards dual-functional wireless networks for 6G and beyond," *IEEE J. Sel. Areas Commun.*, pp. 1–1, early access, 2022, doi: 10.1109/JSAC.2022.3156632.

[3] F. Liu, W. Yuan, C. Masouros, and J. Yuan, "Radar-assisted predictive beamforming for vehicular links: Communication served by sensing," *IEEE Trans. Wireless Commun.*, vol. 19, no. 11, pp. 7704–7719, 2020.

[4] N. Su, F. Liu, Z. Wei, Y.-F. Liu, and C. Masouros, "Secure dual-functional radar-communication transmission: Exploiting interference for resilience against target eavesdropping," *IEEE Trans. Wireless Commun.*, 2022.

[5] G. Li, S. Wang, J. Li, R. Wang, F. Liu, M. Zhang, X. Peng, and T. X. Han, "Rethinking the tradeoff in integrated sensing and communication: Recognition accuracy versus communication rate," *arXiv preprint arXiv:2107.09621*, 2021.

[6] J. Yang, G. Cui, X. Yu, and L. Kong, "Dual-use signal design for radar and communication via ambiguity function sidelobe control," *IEEE Trans. Veh. Technol.*, vol. 69, no. 9, pp. 9781–9794, 2020.

[7] R. Zhang, B. Shim, W. Yuan, M. Di Renzo, X. Dang, and W. Wu, "Integrated sensing and communication waveform design with sparse vector coding: Low sidelobes and ultra reliability," *IEEE Trans. Veh. Technol.*, 2022.

[8] X. Wang, Z. Fei, Z. Zheng, and J. Guo, "Joint waveform design and passive beamforming for ris-assisted dual-functional radar-communication system," *IEEE Trans. Veh. Technol.*, vol. 70, no. 5, pp. 5131–5136, 2021.

[9] E. Fishler, A. Haimovich, R. S. Blum, L. J. Cimini, D. Chizhik, and R. A. Valenzuela, "Spatial diversity in radars—models and detection performance," *IEEE Trans. Signal Process.*, vol. 54, no. 3, pp. 823–838, 2006.

[10] L. Xu, J. Li, and P. Stoica, "Target detection and parameter estimation for MIMO radar systems," *IEEE Trans. Aerosp. Electron. Syst.*, vol. 44, no. 3, pp. 927–939, 2008.

[11] G. Cui, H. Li, and M. Rangaswamy, "MIMO radar waveform design with constant modulus and similarity constraints," *IEEE Trans. Signal Process.*, vol. 62, no. 2, pp. 343–353, 2013.

[12] X. Liu, T. Huang, N. Shlezinger, Y. Liu, J. Zhou, and Y. C. Eldar, "Joint transmit beamforming for multiuser MIMO communications and MIMO radar," *IEEE Trans. Signal Process.*, vol. 68, pp. 3929–3944, 2020.

[13] R. W. Heath, N. Gonzalez-Prelcic, S. Rangan, W. Roh, and A. M. Sayeed, "An overview of signal processing techniques for millimeter wave MIMO systems," *IEEE J. Sel. Topics Signal Process.*, vol. 10, no. 3, pp. 436–453, 2016.

[14] W. Yuan, F. Liu, C. Masouros, J. Yuan, D. W. K. Ng, and N. González-Prelcic, "Bayesian predictive beamforming for vehicular networks: A low-overhead joint radar-communication approach," *IEEE Trans. Wireless Commun.*, vol. 20, no. 3, pp. 1442–1456, 2020.

[15] S. M. Kay, *Fundamentals of statistical signal processing: estimation theory*. Prentice-Hall, Inc., 1993.

[16] S. Rezvani, N. M. Yamchi, M. R. Javan, and E. A. Jorswieck, "Resource allocation in virtualized CoMP-NOMA HetNets: Multi-connectivity for joint transmission," *IEEE Trans. Commun.*, vol. 69, no. 6, pp. 4172–4185, 2021.

[17] S. Boyd, S. P. Boyd, and L. Vandenberghe, *Convex optimization*. Cambridge university press, 2004.